J Solid State Electrochem (2011) 15:2395–2400
DOI 10.1007/s10008-011-1479-4

ORIGINAL PAPER

Layer-by-layer deposition of a polythiophene/Au nanoparticles multilayer with effective electrochemical properties

Barbara Zanfrognini · Chiara Zanardi · Fabio Terzi · Timo Ääritalo · Antti Viinikanoja · Jukka Lukkari · Renato Seeber

Received: 1 May 2011 / Revised: 13 June 2011 / Accepted: 14 June 2011 / Published online: 29 June 2011
© Springer-Verlag 2011

Abstract Multilayers consisting of a water soluble polythiophene derivative and Au nanoparticles have been deposited onto different electrode substrates by means of layer-by-layer deposition technique. The assembly of the films has been performed by taking advantage of the electrostatic interactions between the positively charged imidazolic moiety of the polythiophene chain and the negative charges of citrate ions surrounding Au nanoparticles, as well of the affinity of S to Au. The nanoparticles result stably grafted to the organic matrix. The resulting modified electrodes have been characterised through electrochemical, spectroelectrochemical and microscopic techniques. The results evidenced that a high number of individual nanoparticles is present inside the multilayer. The presence of nanoparticles is of chief importance for most effective charge percolation through the multilayer, as suggested by the responses to electroactive probe species in solution. The electrocatalytic performances of the modified electrodes have been tested with respect to the oxidation of ascorbic acid.

Keywords Nanostructured composites · Polythiophene · Au nanoparticles · Layer-by-layer deposition · Electrocatalysis

B. Zanfrognini · C. Zanardi · F. Terzi · R. Seeber (✉)
Department of Chemistry,
University of Modena and Reggio Emilia,
via G. Campi 183,
41125 Modena, Italy
e-mail: renato.seeber@unimore.it

T. Ääritalo · A. Viinikanoja · J. Lukkari
Department of Chemistry and Turku University Centre
for Materials and Surfaces (MATSURF), University of Turku,
FIN-20014 Turku, Finland

Introduction

A notable portion of the investigations in the field of electroanalysis is nowadays oriented toward the development of hybrid materials consisting of metal functionalities inserted into organic matrices [1–9]. In particular, metal ions, clusters and nanoparticles of different nature can be profitably inserted into redox or conducting polymers by taking advantage of the synergic properties of the organic and the inorganic components. In similar systems, the presence of the metal deeply affects the electronic and electrochemical properties of the resulting hybrid material, possibly improving the performances with respect to the pure organic component.

By considering the organic component, polythiophene derivatives (PTs) constitute the most extensively used class of conducting polymers in the field of the electrochemical sensors. Although PTs cannot be considered strictly reversible redox mediators, they constitute interesting alternatives to conventional electrode surfaces; in particular, they can reduce the overvoltage of inner sphere non-reversible charge transfer, they posses high electrochemical, mechanical and thermal stability, as well as antifouling and electrocatalytic capabilities [10, 11]. Moreover, the possibility to introduce specific functional groups into the monomer unit, i.e. along the polymeric chain, widens the range of accessible electrode modifications suitable for realising amperometric- and potentiometric-sensing systems.

The possibility to introduce metal centres of different nature into the polymer matrix constitutes a potentially powerful way to further improve the electrocatalytic performance of the electrode. Considering the inorganic counterpart, the Au nanoparticles (AuNPs) are particularly promising in the amperometric sensing. The peculiar

catalytic characteristics of the NPs are ascribable to the high surface-to-volume ratio and to the polyhedral shape of the particles, which lead to a high percentage of atoms located in correspondence of "structural defects", i.e., at edges and vertexes, hence possessing unsaturated coordination [12–14]. Furthermore, the properties of AuNPs can be tuned by varying the metal core diameter and the nature of the surrounding organic shell. When designing effective electrocatalytic coatings based on AuNPs, a high density of isolated nanoparticles at the electrode/solution interface should be incorporated; in addition, the metal nanoparticles should interact with species in solution.

In previous works [15, 16], the organic component coupled to the AuNPs consisted of a redox polymer, which is electroactive in a narrow, cathodic potential range and can incorporate AuNPs by electrostatic and Au–N interactions. On the other hand, PTs appear well suited for the organic component in the AuNPs/polymer composite films. The S atoms induce stable interaction with the metal cores and the three-dimensional polymeric structure allows the deposition of a large number of AuNPs avoiding the coalescence of the metal cores. This last aspect is of special importance in order to exploit their electrocatalytic properties.

A wide number of chemical or electrochemical approaches have been developed to synthesise PT/AuNP composite materials [1, 17–19]. With this respect, it should be taken in account that when the synthesis of both components is carried out through a chemical approach, the pure organic and inorganic materials can be exhaustively characterised, and many composite coatings can be deposited from a single synthetic stock. As a direct consequence, a higher reproducibility in the formation of the coating can be obtained.

In view of all the aspects previously discussed, the layer-by-layer (LbL) deposition technique constitutes a versatile and simple method for the formation of composite layers with the characteristics sought. The procedure, first developed by Decher [20, 21], is based on the electrostatic interaction between oppositely charged species, which are adsorbed by sequential immersion of the substrate in the solutions of the two components. The advantage of this deposition procedure lies in the easy formation of a coating with tuneable physico-chemical properties, depending on the nature of the polyelectrolytes, the number of layers deposited and the experimental conditions adopted [22]. The method, firstly applied to polyelectrolytes, can be extended to a variety of materials including metal and metal oxide NPs surrounded by a charged organic shell, proteins and enzymes.

We present here a study on the growth and characterisation of a multilayer consisting of a PT derivative, namely poly(1-methyl-3-[3-[3-thienyloxy]-propyl]-1*H*-imidazolium) fluoride (P3TOPIM), reported in Scheme 1 [23] and AuNPs encapsulated by citrate ions ($AuNP_{citr}$). The polymer was synthesised in order to carry a positive charge that can be exploited for LbL assembly. $AuNP_{citr}$ can be easily obtained by a large-scale synthesis leading to NPs characterised by a narrow dimensional distribution and good long-term stability, as suggested by transmission electron microscope (TEM) and UV–Vis analyses [15]. In addition, the lability of the citrate-encapsulating agent allows good accessibility of the electroactive species to the metal core.

Experimental

Chemicals

All reagents were of pure or puriss. grade (Aldrich) and used as received. All aqueous solutions were prepared with Millipore water, 18-MΩ-cm resistivity. The synthesis and characterisation of P3TOPIM is reported elsewhere [23]. $AuNP_{citr}$ were synthesised in the presence of citrate ions as the encapsulating agent, according to refs. [15, 24]. The metal core mean diameter was calculated to be 14±1 nm, on the basis of TEM images.

Multilayer build-up

Multilayer films were built by alternatively dipping the proper substrate in aqueous solutions of P3TOPIM and $AuNP_{citr}$, up to ten bilayers. The number of bilayers and the deposition conditions were properly chosen on the basis of previous studies [15], in order to obtain a homogeneous film, completely covering the electrode surface. The LbL assembly of the $(P3TOPIM/AuNP_{citr})_{10}$ multilayers was performed on a 2-mm Au electrode or on indium tin oxide (ITO) substrates. The Au electrode (Metrohm) was cleaned with 1- and 0.3-μm alumina powder and then rinsed with ultra-pure water in an ultrasonic bath for 5 min. The procedure was completed by cycling the electrode between −0.20 and +1.15 V vs. saturated $Hg/HgSO_4$ (Amel) at 0.1 Vs^{-1} potential scan rate, in 0.5 M H_2SO_4 solution, until a repeatable cyclic voltammogram, typical of a clean Au electrode, was obtained. The bare Au surface was, then, negatively charged by 30 min immersion in a 1-mM sodium 2-mercaptoethanesulfonate (MESA) aqueous solu-

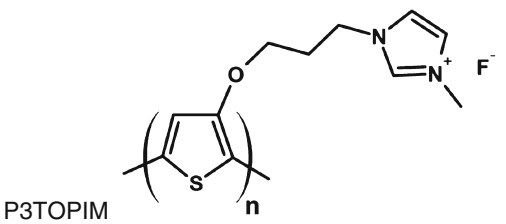

Scheme 1 Chemical structure of poly(1-methyl-3-[3-[3-thienyloxy]-propyl]-1*H*-imidazolium)fluoride

tion. As to ITO, the surface was cleaned with ethanol in an ultrasonic bath for 10 min, renewing the bath after 5 min. The side opposite to the ITO surface was coated by Teflon tape in order to prevent from any depositions; only the conductive ITO-coated side resulted hence negatively charged by immersion in a 98% H_2SO_4/96% EtOH 1:1 mixture for 1 h, at room temperature. The $(P3TOPIM/AuNP_{citr})_{10}$ multilayers were built on the negatively charged surfaces by alternatively dipping the substrate in the cationic P3TOPIM (1.0 mg/ml in 0.01 M phosphate buffer solution, PBS, pH 7.0) solution for 20 min and in the anionic $AuNP_{citr}$ (0.087 mg_{Au}/ml in 0.001 M PBS) solution for 3 min. After every deposition step, the substrate was carefully rinsed with ultra-pure water and immersed in a water bath for 1 min. Although the growth of the films has been carried out on different surfaces, viz. Au and ITO, based on our previous experience, we can assume that the electrochemical behaviours of the multilayers obtained in the two cases are quite similar and, thus, comparable [15]. This assumption can be reasonably accepted when aiming at a non-quantitative estimation of the amount of deposited material, i.e. when one only needs checking the effectiveness of the deposition.

Multilayer characterisation

Electrochemical tests were performed with an Autolab PGSTAT12 (Ecochemie) potentiostat/galvanostat equipped with a Metrohm 663 VA stand. The electrochemical cell consisted of a 2-mm diameter Au-working electrode, a glassy carbon rod auxiliary electrode (Metrohm) and an aqueous Ag/AgCl, 3 M KCl reference electrode (Amel). All potential values given are referred to this reference electrode. Cyclic voltammetry (CV) experiments were carried out in 0.1 M PBS containing $[Fe(CN)_6]^{4-}$, $[Ru(NH_3)_6]^{3+}$ or ascorbic acid (AA) as electroactive species.

Spectroelectrochemical tests were performed by coupling the potentiostat to an UV–Vis Lambda 650 (Perkin Elmer) spectrophotometer, operating in the spectral range between 350 and 900 nm. In this case, the electrochemical cell was directly assembled inside the quartz cuvette; the working electrode was an ITO glass slide, a home-made Ag/AgCl, 3 M KCl was the reference electrode, while the auxiliary electrode consisted of a Pt wire.

TEM images were acquired using a JEOL 2010 instrument, equipped with an energy filter (Gatan Inc.) and an energy-dispersive spectrometer (EDS-INCA system, Oxford Instruments). Au TEM grids, cleaned in advance with piranha solution (98% H_2SO_4/30% H_2O_2 7:3 mixture) and coated by a MESA layer, have been used for the growth of the multilayers. The grids have been alternatively dipped in the solutions of the two components and dried in air for at least 10 min. The images of the multilayer were acquired at the film/ambient interface along the edges of an Au grid modified with the multilayer. In particular, images were obtained focusing the beam on the edge of the film, in correspondence to particularly thin regions of the multilayer. The analyses were performed by cooling the walls of the sample chamber at liquid nitrogen temperature in order to minimise contamination.

Results and discussion

The growth of the multilayer on ITO surface was followed by recording the UV–Vis spectra after the deposition of each $P3TOPIM/AuNP_{citr}$ bilayer, as reported in Fig. 1. These measurements take advantage of absorption bands typical of the two components of the film, namely the AuNPs plasmon band and the π-π^* transition band of the polymer, both bands being located in the visible region and strongly overlapping each other. As shown in the inset of Fig. 1, the intensity of the UV–Vis absorption increases with increasing the number of bilayers, confirming the growth of the film. Although the deconvolution of the PT absorption band and of the AuNP plasmon band from the overall broad band centred at ca. 530 nm is quite difficult, it could be shown that the contribution to the absorbance due to the $AuNP_{citr}$ is about two orders of magnitude higher than that of PT (see hereafter). In view of this, some considerations can be made about the state of the NPs inside the composite by considering the position of λ_{max}. In particular, the small extent of the red-shift with respect to the spectrum of NPs in solution ($\Delta\lambda \approx 10$ nm) is compatible with NPs close to each other, however, retaining their individuality. Metal core coalescence phenomena would result in a much more marked λ_{max} red-shift in the spectra. The small shift observed has been, in fact, already found for different multilayers containing metal NPs [15, 25–27] and can be ascribed to NPs grafted on solid surfaces. The shift is caused by the coupling of the plasmon oscillations, which is due to the lowering of the average distance between adjacent NPs. Moreover, a slight shift of the band maximum towards higher wavelength, due to the change of the dielectric constant of the medium surrounding the metal cores, has to be taken into account [28].

These considerations are definitely confirmed by TEM images; one of these is reported in Fig. 2 as a representative example. The formation of a composite, in which NPs are dispersed inside the polymeric matrix, is well evident in the TEM images. These testify that the multilayer growth does not lead to a significant NP coalescence, as discussed above for the UV–Vis characterisation. The NP mean diameter inside the composite (14±1 nm) is equal to that observed for individual NP metal cores in solution, immediately after the synthesis. The NPs appear erroneously overlapped due to the projection of the three-dimensional structures onto

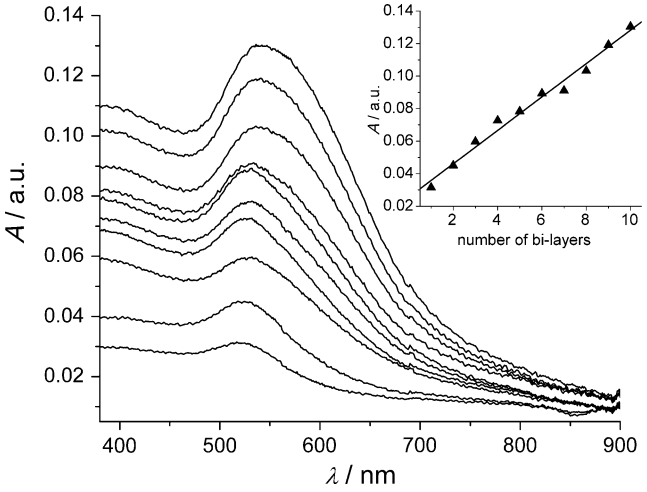

Fig. 1 UV–Vis spectra registered after the deposition of each of the ten subsequent (P3TOPIM/$AuNP_{citr}$) bilayers onto an ITO glass slide. The spectra have been corrected for the absorption of the bare substrate. The maximum absorbance value vs. the number of bilayers plot is reported in the inset–correlation coefficient=0.992

the detector plane. By suitable variation of the instrumental parameters of the microscope—in particular of the focal plane—it is possible to show that NPs apparently close to each other are, in fact, located on different planes. Moreover, it is well known that NPs can self-assemble on a surface leading to bi- and tridimensional structures with hexagonal symmetry; these structures can be inferred from an analysis of the TEM images.

Once deposited onto the ITO glass slide, the composite was characterised by a spectroelectrochemical technique, which allows the analysis of the UV–Vis absorption spectra at different applied potentials. After 100 s of electrode polarisation, several spectra were acquired in order to verify that the polymer has reached the steady state. Figure 3 shows the second UV–Vis spectrum registered for each

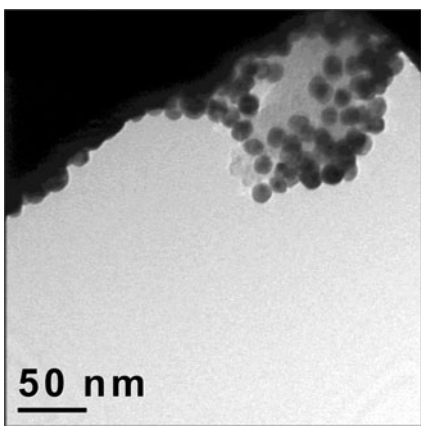

Fig. 2 TEM image at the film/ambient interface of a (P3TOPIM/$AuNP_{citr}$)$_{10}$ multilayer

investigated potential (+0.40, +0.60 and +0.70 V); the spectrum registered at the potential of +0.0 V was subtracted in all cases. The presence of an isosbestic point suggests that two main species are involved, one being converted into the other. The absorption related to the neutral chain, centred at ca. 570 nm, decreases at increasing the potential. This decrease is associated to the concomitant increase of a band located at wavelengths higher than 680 nm, corresponding to one of the two electronic transitions of the polaronic form [29–31]. The very small absorbance variation due to PT oxidation suggests that the contribution of P3TOPIM bands to the overall absorbance is quite low with respect to that of the AuNPs plasmon band. Considering that the relevant mass extinction coefficients in solution are of the same order of magnitude, we can conclude that only a small amount of polymer is present in the coating, in comparison to that of NPs. The almost perfect overlap between the initial spectrum and the spectrum registered after repolarising the electrode again at +0.0 V shows that polymer p-doping is a completely reversible process in these composite films.

Spectroelectrochemical tests using cyclic voltammetry were also performed on the composite coating by monitoring the absorbance at λ=570 nm. This wavelength value was selected because it presents the maximum absorption variation of the neutral form of the polymer at the different applied potentials. Figure 4 reports the absorbance values registered while cycling the ITO electrode modified with the composite film in the range −0.2 to +0.8 V at 0.005 Vs^{-1} potential scan rate. As expected, during the forward scan, a

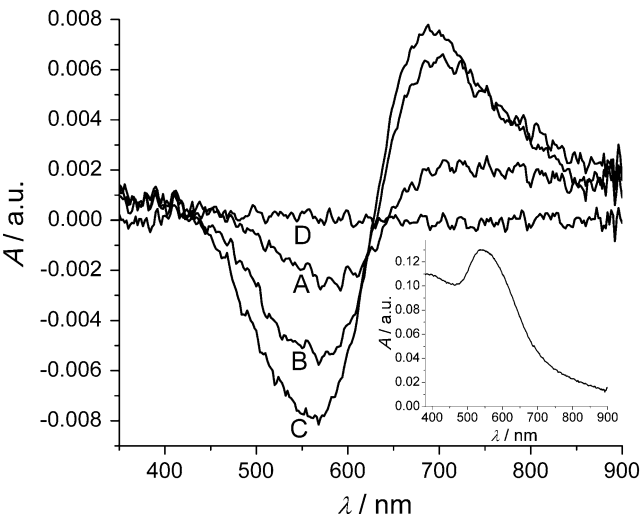

Fig. 3 UV–Vis spectra registered for a (P3TOPIM/$AuNP_{citr}$)$_{10}$-modified ITO glass slide, polarised at different potentials; to all spectra that registered at the potential of 0.0 V has been subtracted. *A* +0.4 V; *B* +0.6 V; *C* +0.7 V; *D* 0.0 V backward. In the *inset*, UV–Vis spectrum of (P3TOPIM/$AuNP_{citr}$)$_{10}$-modified ITO glass slide, polarised at 0.0 V, is reported

decrease of the absorption intensity is observed due to a progressive oxidation of P3TOPIM on the electrode surface. The absorbance reaches a minimum in correspondence to the switching potential of each cycle. Then, in the backward scan, P3TOPIM is gradually reduced back to the neutral form, and the absorbance shows a complete recovery of the original value, proving the stability of the film on the electrode surface. It is worth noticing that the variation of the maximum absorbance in the different subsequent cycles is very low in agreement to what was already observed in Fig. 3 under steady-state conditions.

The behaviour of the modified electrode was tested with benchmark electroactive species undergoing uncomplicated charge transfer, namely $[Ru(NH_3)_6]Cl_3$ and $K_4[Fe(CN)_6]$, chosen as reversibly reducible and oxidisable species, respectively. Figure 5a shows the comparison between the voltammetric response of the $(P3TOPIM/AuNP_{citr})_{10}$-modified electrode and bare Au in a 5 mM $K_4[Fe(CN)_6]$, 0.1 M PBS. The increase of the peak current in the former case is observed although negative cloud surrounding AuNPs at the external layer of the coating could be expected to oppose the transfer of $[Fe(CN)_6]^{4-}$ ions to the electrode. This phenomenon can be accounted for by the increase of the electroactive area due to the surface roughness induced by the AuNPs ensembles shown in the TEM images, whose dimensions are much higher than the diffusion layer thickness in the time scale of the measurement. Similar features are observed in the voltammetric response of $[Ru(NH_3)_6]Cl_3$ solutions. The voltammetric traces (data not shown) for both electroactive species, registered at different potential scan rates between 0.005 and 0.400 Vs^{-1}, exhibit peak-to-peak separations close to 60 mV, which indicates a negligible ohmic drop inside the coating. Moreover, a linear dependence of the peak current on the square root of the potential scan rate implies, in both cases, a diffusion-controlled charge transfer process. It is worth noticing that in case of the $[Ru(NH_3)_6]Cl_3$ electroreduction process, AuNPs are well effective in favouring charge percolation throughout the whole film, despite the insulating character of the polymer matrix at these cathodic potentials.

In order to study the behaviour of the electrode coating in case of more complex, irreversible charge transfer process, the properties of the multilayer were tested in the oxidation of AA in PBS. In Fig. 5b, the voltammetric traces registered at bare and modified Au electrodes in a 3-mM AA solution are

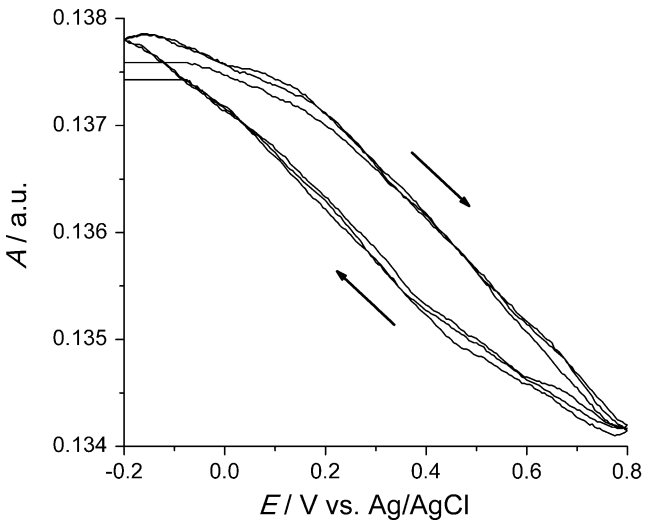

Fig. 4 Absorbance values registered at λ=570 nm at different applied potentials of a CV experiment in 0.1 M PBS; three scans at 0.005 Vs^{-1} potential scan rate (filtered data)

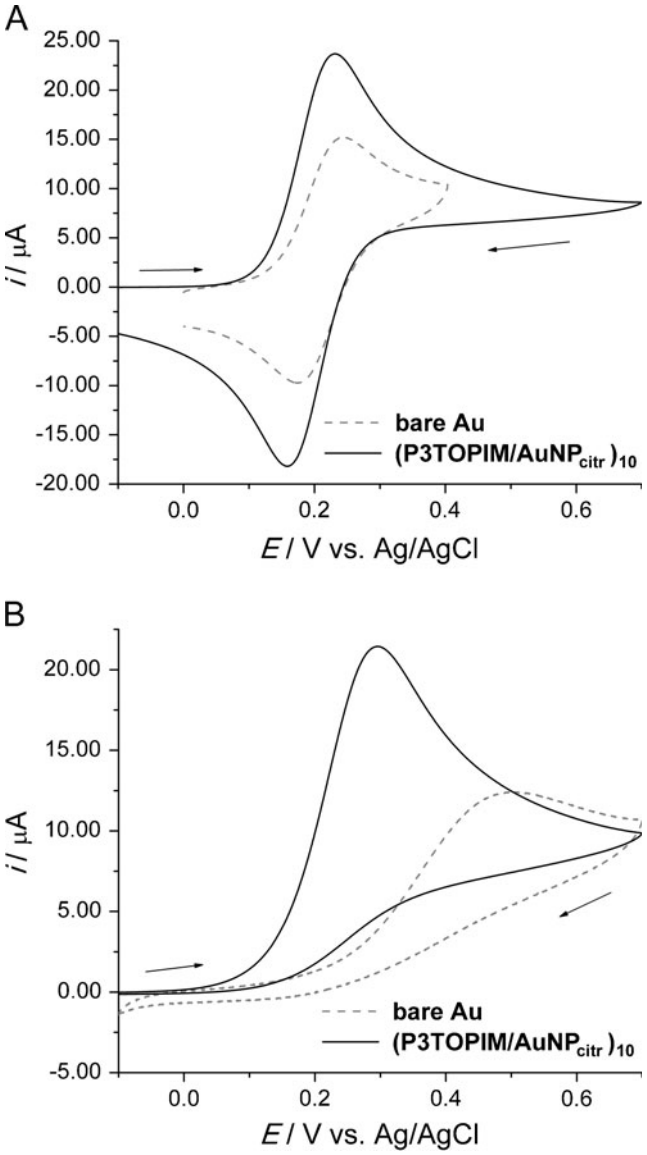

Fig. 5 Comparison between CV responses registered at a $(P3TOPIM/AuNP_{citr})_{10}$ modified and at a bare Au electrode in (**a**) 5-mM $K_4[Fe(CN)_6]$ and (**b**) 3-mM AA solutions in 0.1 M PBS; steady-state voltammograms are reported; 0.050 Vs^{-1} potential scan rate

compared. The CV responses clearly imply much better performance of the modified electrode in the electrocatalytic oxidation of AA compared to bare Au [32], in terms of (a) lower oxidation potential, (b) higher current density and (c) peak sharpness, which is diagnostic of effective electrocatalytic effect. Furthermore, since the anodic oxidation of such a species is known to involve poisoning due to the adsorption of reaction intermediates, the composite should be also acknowledged to posses interesting antifouling properties.

Conclusions

The LbL deposition technique was successfully employed to build up a composite electrode coating consisting of AuNPs stably anchored between polythiophene layers. Although the amount of polymer is found to be low, it allows the deposition of a high number of AuNPs preserving their own individuality, hence exploiting at best their electrocatalytic properties. The electrochemical behaviour of the coating indicates that the electroactive area of the modified electrode is significantly enhanced with respect to the bare Au surface and that the charge transfer throughout the film is mainly due to the high amount of AuNPs inside the composite. The electrocatalytic properties of the coating were tested toward the electrooxidation of AA; the effectiveness of the modified electrode with respect to such a critical oxidation process encourages the possible application of this kind of electrode system as amperometric sensors for further analytes, even in real matrices. Nevertheless, tests on additional possible electroactive species undergoing different complex electrode mechanisms are beyond the scope of the present article and are not conducted in this context.

References

1. Zanardi C, Terzi F, Pigani L, Seeber R (2011) In: Lechkov M, Prandzheva S (eds) Encyclopedia of polymer composites: properties, performance and applications. Nova, New York
2. Gómez-Romero P, Sanchez C (2004) Functional hybrid materials. Wiley, Weinheim
3. Tsakova V, Ivanov S, Lange U, Stoyanova A, Lyutov V, Mirsky VM (2011) Pure Appl Chem 83:345–358
4. Welch CM, Compton RG (2006) Anal Bioanal Chem 384:601–619
5. Campbell FW, Compton RG (2010) Anal Bioanal Chem 396:241–259
6. Hernandez-Santos D, Begona Gonzalez-Garcia M, Costa Garcia A (2002) Electroanal 14:1225–1235
7. de Dios AS, Díaz-García MA (2010) Anal Chim Acta 666:1–22
8. Pandey P, Arya SK, Matharu Z, Singh SP, Datta M, Malhotra DB (2008) J Appl Pol Sci 110:988–994
9. Chirea M, García-Morales V, Manzanares JA, Pereira C, Gulaboski R, Silva F (2005) J Phys Chem B 109:21808–21817
10. McQuade DT, Pullen AE, Swager TM (2000) Chem Rev 100:2537–2574
11. Heinze J, Frontana-Uribe BA, Ludwigs S (2010) Chem Rev 110:4724–4771
12. Sau TK, Rogach AL, Jackel F, Klar TA, Feldmann J (2010) Adv Mater 22:1805–1825
13. Roucoux A, Schulz J, Patin H (2002) Chem Rev 102:3757–3778
14. Daniel MC, Astruc D (2004) Chem Rev 104:293–346
15. Terzi F, Zanardi C, Zanfrognini B, Pigani L, Seeber R, Lukkari J, Ääritalo T, Kankare J (2009) J Phys Chem C 113:4868–4874
16. Zanardi C, Terzi F, Zanfrognini B, Pigani L, Seeber R, Lukkari J, Ääritalo T (2010) Sens Act B 144:92–98
17. Zotti G, Vercelli B, Berlin A (2008) Acc Chem Res 41:1098–1109
18. Antolini E, Gonzalez ER (2009) Appl Cat A 365:1–19
19. Tarushee Ahujab R, Kumarb D (2009) Sens Act B 136:275–286
20. Decher G (1997) Science 277:1232–1237
21. Decher G, Schlenoff JB (2003) Multilayer thin films: sequential assembly of nanocomposite materials. Wiley, Weinheim
22. Dubas ST, Schlenoff JB (1999) Macromolecules 32:8153–8160
23. Viinikanoja A, Areva S, Kocharova N, Ääritalo T, Vuorinen M, Savunen A, Kankare J, Lukkari J (2006) Langmuir 22:6078–6086
24. Turkevich J, Stevenson PC, Hillier J (1951) Discuss Faraday Soc 11:55–75
25. Jiang C, Markutsya S, Tsukruk VV (2004) Langmuir 20:882–890
26. Moores A, Goettmann F (2006) New J Chem 30:1121–1132
27. Ung T, Liz-Marzán LM, Mulvaney O (2001) J Phys Chem B 105:3441–3452
28. Underwood S, Mulvaney P (1994) Langmuir 10:3427–3430
29. Pern FJ, Frank AJ (1990) J Electrochem Soc 137:2769–2777
30. Bredas JL, Street GB (1985) Acc Chem Res 18:309–315
31. Patil AO, Heeger AJ, Wudl F (1988) Chem Rev 88:183–200
32. Murthy ASN, Sharma J (1998) Anal Chim Acta 363:215–220